

For the case illustrated in Fig. 7, the numerically computed inflection points occur at

$$h_{qp}^z = 1.990, \quad \phi_{qp}^z = 74.44^\circ,$$

$$h_{qp}^x = 2.195, \quad \phi_{qp}^x = 74.97^\circ,$$

where $h_K=0$, $h_L=0.1$, $h_D=0.05$. Equations (30) and (31) give

$$h_{qp}^z = 2.009, \quad \phi_{qp}^z = 74.0^\circ,$$

$$h_{qp}^x = 2.212, \quad \phi_{qp}^x = 74.5^\circ.$$

V. CONCLUSION

The addition of a DM interaction to the uniaxial antiferromagnet with anisotropic exchange yields a Heisenberg isotropic exchange Hamiltonian with general second-order anisotropy. The hysteresis of the first-order spin-flop transition is reduced as \mathbf{D} is increased and the paramagnetic transition only occurs when the field is applied parallel to \mathbf{D} . Experimentally, a quasi-paramagnetic transition would be observed as an inflection point in the susceptibility for fields not parallel to \mathbf{D} .

* Work supported by a National Science Foundation grant.

† NDEA Title IV Fellow.

¹ T. Nagamiya, K. Yosida, and R. Kubo, *Advan. Phys.* **4**, 1 (1955).

² H. Rohrer and H. Thomas, *J. Appl. Phys.* **40**, 1025 (1969).

³ J. Feder and E. Pytte, *Phys. Rev.* **168**, 640 (1968).

⁴ F. B. Anderson and H. B. Callen, *Phys. Rev.* **136**, A1068 (1964).

⁵ T. Moriya, *Phys. Rev.* **120**, 91 (1960).

⁶ G. Cinader, *Phys. Rev.* **155**, 453 (1966).

⁷ M. S. Seehra and T. G. Castner, *Phys. Rev. B* **1**, 2289 (1970).

⁸ K. P. Belov, A. M. Kadomtseva, and R. Z. Bevitin, *Zh. Exprim. i Teor. Fiz.* **51**, 1306 (1966) [*Soviet Phys. JETP* **24**, 878 (1967)].

⁹ E. F. Bertaut, in *Magnetism*, edited by G. T. Rado and H. Shul (Academic, New York, 1963) Vol. III.

¹⁰ K. W. Blazey *et al.*, *Phys. Rev. Letters* **24**, 105 (1970).

¹¹ J. E. Rives, *Phys. Rev.* **162**, 491 (1967).

Effects of Hydrostatic Pressure and of Jahn-Teller Distortions on the Magnetic Properties of RbFeF_3 †

J. B. GOODENOUGH, N. MENYUK, K. DWIGHT, AND J. A. KAFALAS

Lincoln Laboratory, Massachusetts Institute of Technology, Lexington, Massachusetts 02173

(Received 19 June 1970)

The first-order transitions at $T_1=40^\circ\text{K}$ and $T_2=87^\circ\text{K}$ in RbFeF_3 have been measured as a function of hydrostatic pressure and applied magnetic field. It was not possible to observe the $T_N=102^\circ\text{K}$ transition with a magnetic-susceptibility measurement. It was found that $(\Delta T_1/\Delta H_a)_p=0.35^\circ/\text{kOe}$, $(\Delta T_2/\Delta H_a)_p=0.19^\circ/\text{kOe}$, $(\Delta T_1/\Delta P)_H=0.18^\circ/\text{kbar}$ and $(\Delta T_2/\Delta P)_H=-0.81^\circ/\text{kbar}$. These results correspond to latent heats of 0.006 and 0.04 cal/g at T_1 and T_2 , respectively, and relative volume changes $\Delta V_1/V_1=1.5\times 10^{-6}$, $\Delta V_2/V_2=-22\times 10^{-6}$. It is pointed out that a Jahn-Teller distortion to tetragonal ($c/a>1$) symmetry in the interval $T_2<T<T_N$ introduces a strong magnetoelastic coupling. This causes the heavy twinning that has been observed below T_N , and the resulting twinned structure is retained in the entire temperature interval $0<T<T_N$. In the temperature interval $T_1<T<T_2$, $\text{Rb}^+\text{-F}^-$ interactions induce distortions to orthorhombic or tetragonal symmetries that are superimposed on the Jahn-Teller distortion. The orthorhombic distortion is cooperative across twin boundaries caused by the Jahn-Teller distortion and also permits spin canting, which introduces a ferromagnetic component below T_2 . It is shown how the interplay of these distortions plus strong magnetoelastic coupling can explain the appearance of two sets of Mössbauer peaks below T_2 and results in macroscopic ferromagnetic components having cubic symmetry even though the microscopic crystallographic symmetry is "orthorhombic" ($T_1<T<T_2$). The Jahn-Teller distortion changes to rhombohedral ($\alpha<60^\circ$) for $T<T_1$; in combination with the existing orthorhombic structure, this produces monoclinic symmetry on a microscopic scale. Nevertheless, it is shown that the macroscopic magnetization retains its cubic symmetry, that the easy magnetization direction changes from $\langle 100 \rangle$ to the $\langle 110 \rangle$, that the apparent moment increases, and that there may still be two sets of Mössbauer peaks.

I. INTRODUCTION

Above its Néel temperature $T_N=102^\circ\text{K}$,¹ RbFeF_3 has the cubic perovskite structure, but it becomes tetragonal ($c/a>1$) in the interval $T_2<T<T_N$.² It undergoes first-order transitions at $T_1=40^\circ\text{K}$ and $T_2=87^\circ\text{K}$; it exhibits weak ferromagnetism at all $T<87^\circ\text{K}$.³ In the interval $T_1<T<T_2$, the structure appears to be

orthorhombic, and below T_1 it has lower symmetry, probably monoclinic.² The ferromagnetic moment has a preferred direction along the pseudocubic $\langle 100 \rangle$ axes in the interval $T_1<T<T_2$, along the pseudocubic $\langle 110 \rangle$ axes below T_1 .⁴ It is remarkable that these noncubic crystals exhibit a cubic macroscopic anisotropy of the weak ferromagnetism. A neutron-diffraction study on a polycrystalline sample shows the dominant magnetic

structure to be a simple type-G antiferromagnet for all $T < T_N$.⁵ However, Mössbauer measurements below T_2 distinguish two types of iron sites, and this finding was claimed to be incompatible with a simple canting of the spins to produce the weak ferromagnetism.¹

The transition temperatures T_1 and T_2 both vary with applied magnetic field H_a . Wertheim *et al.*¹ obtained a shift of T_2 to 95°K and of T_1 to 45°K in an $H_a=14\,240$ Oe, corresponding to a $\Delta T_2/\Delta H_a=0.56^\circ/\text{kOe}$ and a $\Delta T_1/\Delta H_a=0.35^\circ/\text{kOe}$. Testardi *et al.*,² on the other hand, required a field of 4 kOe to achieve a $\Delta T_2 \approx 0.5^\circ\text{K}$, corresponding to a $\Delta T_2/\Delta H_a \approx 0.125^\circ\text{K}$. No discussion was given of the rather striking difference in the two results.

In this paper we report studies of the magnetic properties of RbFeF_3 in the vicinity of the first-order transformations as functions of both applied field and hydrostatic pressure. We also present a microscopic interpretation of the magnetic and crystallographic data.

II. EXPERIMENTAL

The powder sample used in these measurements was obtained by grinding a single crystal grown by O'Connor. The starting material was obtained from the reaction of high-purity RbF and FeCl_2 heated in a graphite crucible to 1000°C. RbCl was removed from the product by dissolving in water. Crystals were grown from the melt in a graphite crucible contained in a sealed nickel crucible, with provision for adding a small amount of NH_4HF_2 . A sharp temperature gradient provided optimum growth conditions.

The measurements were performed on a vibrating-coil magnetometer used in conjunction with a helium-gas pressure-generating unit. This system permits the direct measurement of magnetic moment while freely varying applied field, temperature, and pressure.⁶

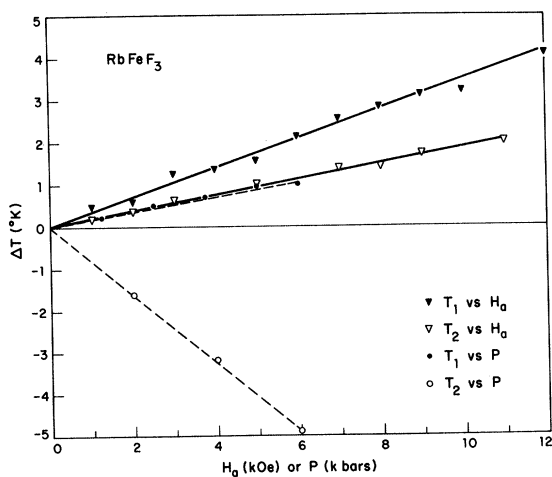


FIG. 1. Changes in the RbFeF_3 transition temperatures T_1 and T_2 as functions of applied magnetic field strength H_a or hydrostatic pressure P .

TABLE I. Parameters of the two first-order transitions in RbFeF_3 .

T_i (°K)	$(\partial T_i/\partial H)_P$ (deg/kOe)	$(\partial T_i/\partial P)_H$ (deg/kbar)	L_i (cal/g)	$(\Delta V_i/V_i)$ ($\times 10^6$)
41	0.35	0.18	0.006	1.5
87	0.19	-0.81	0.04	-22

The magnetization-versus-temperature curve closely approximated that given by Wertheim *et al.*,¹ except that our measured saturation moment at 4.2°K was approximately 14.5 emu/g rather than the 16 emu/g they obtained. This 10% drop can be explained by the fact that our measurements were taken on a polycrystalline sample in fields up to $H_a=12$ kOe, since the anisotropy investigations of Gyorgy *et al.*⁴ indicate that at these applied fields the magnetization is limited to the easy-axis direction closest to the field. The magnetization curve is characterized by a pronounced step at T_1 .

Investigation of the magnetization in the temperature range $90 \leq T \leq 120^\circ\text{K}$ and in fields $1 < H_a \leq 10$ kOe at both atmospheric pressure and at 5 kbar showed no observable kink in the magnetization-versus-temperature curves in the vicinity of T_N . This accords with the results of Wertheim *et al.*¹ and supports their conclusion that lattice strains produced by crystallographic distortions accompanying short-range magnetic order give rise to a spatial variation of T_N .

Magnetic-moment measurements in the vicinity of the two first-order transitions showed that application of hydrostatic pressure, though shifting T_1 and T_2 , induced no significant change in the magnitudes of the weak ferromagnetic components as a function of $(T_1 - T)$ or $(T_2 - T)$, where $T_1 \approx 41^\circ\text{K}$ in our sample. The variations of T_1 and T_2 with pressure and applied field were found to be linear for pressures $1 < P < 6$ kbar and fields $1 < H_a < 12$ kOe. The results of several measurements are shown in Fig. 1. The resultant slopes are listed in Table I. We found a $\Delta T_1/\Delta H_a \approx 0.35^\circ/\text{kOe}$, in good agreement with that implicit in the data of Wertheim *et al.*¹ The measured sharp increases in ferromagnetic moment $\Delta\sigma_1$ and $\Delta\sigma_2$ on cooling through the transitions at T_1 and T_2 were found to be 2.0 and 3.5 emu/g, respectively. The latter value differs significantly from the 5 emu/g obtained by Testardi *et al.*² Substitution of these values into the Clausius-Clapeyron equations

$$\left(\frac{\partial T}{\partial H_a}\right)_P = -\frac{\Delta\sigma_i}{L_i} T_i \quad \text{and} \quad \left(\frac{\partial T}{\partial P}\right)_{H_a} = \frac{\Delta V_i}{L_i} T_i \quad (1)$$

permits determination of the latent heats L_i and volume changes ΔV_i associated with each of these transitions. These are also listed in Table I. The negative value of ΔV_2 indicates a volume expansion on cooling through the $T_2=87^\circ\text{K}$ transition. The relative volume changes $\Delta V_i/V_i$ are seen to be quite small, probably falling

below the sensitivity of an x-ray determination. The latent heats L_i are also small: The values given in Table I correspond to approximately 0.4 and 3 cm⁻¹/molecule at T_1 and T_2 , respectively.

These small changes are consistent with a microscopic model for the transitions in which magnetoelastic forces play a critical role in determining the relative stabilities of the phases. Indeed, it is notable that $\Delta V_2/V_2$ is comparable to the magnetostrictive strain observed at 77°K.⁴

III. INTERPRETATION

In a cubic crystalline field, octahedral-site Fe²⁺ ions have a threefold-degenerate ${}^5T_{2g,1}(t_{2g}^4e_g^2)$ ground state even after spin-orbit coupling has been included. Since the ground state is not a Kramers doublet, the energy is reduced by a Jahn-Teller distortion to lower point symmetry at lower temperatures. Distortions of the octahedra to either tetragonal or trigonal symmetry can remove the degeneracy. It is customary to define the noncubic component of the crystalline-field energy as

$$V_{nc} = \delta(L_z^2 - \frac{2}{3}), \quad (2)$$

where δ may be either positive or negative. In the case of octahedral-site Fe²⁺ ions, a $\delta < 0$ corresponds to a tetragonal ($c/a > 1$) or a trigonal ($\alpha < 60^\circ$) distortion that stabilizes a Kramers doublet without quenching the spin-orbit-coupling energy. A $\delta > 0$, on the other hand, reverses the signs of the distortions and stabilizes a singlet state, thereby quenching the spin-orbit coupling. If a Jahn-Teller distortion occurs above a magnetic-ordering temperature, a distortion having $\delta > 0$ is stabilized, since distortions that conserve the spin-orbit coupling are not cooperative when the spins are disordered, whereas the elastic coupling between neighboring interstices strongly favors cooperative distortions. On the other hand, if there is no distortion above T_N , then there will be a distortion having $\delta < 0$ at those temperatures $T < T_N$ where the spins are aligned collinearly. Here the magnetic order provides the long-range order that ensures a cooperative elastic distortion if the spin-orbit coupling is not quenched.

It can be shown⁷ that the spectroscopic splitting factor for the effective spin $S' = 1$ has the components

$$\begin{aligned} g_{\parallel} &= (3 + \frac{1}{2}k_c) + 0.52(1 + \frac{1}{2}k_c)(\delta/3k_c\lambda), \\ g_{\perp} &= (3 + \frac{1}{2}k_c) - 0.26(1 + \frac{1}{2}k_c)(\delta/3k_c\lambda), \end{aligned} \quad (3)$$

where $k_c \approx 0.9$ is a factor that takes account of covalent mixing and $\lambda < 0$ is the spin-orbit-coupling constant for the atomic Fe²⁺ ion. In the magnetically ordered state, the internal field \mathbf{H}_i produces a Zeeman splitting

$$\mu_B \mathbf{H}_i \cdot \vec{g} \cdot \mathbf{S}' = (\psi_\theta, H_Z \psi_\theta), \quad (4)$$

where the Zeeman energy is

$$H_Z = \mu_B \mathbf{H}_i \cdot (-k_c \mathbf{L} + 2\mathbf{S}). \quad (5)$$

Therefore, the Zeeman splitting in the molecular fields

is maximized by making $(\delta/\lambda) > 0$ so that g_{\parallel} increases and g_{\perp} decreases. Since $\lambda < 0$, this means a $\delta < 0$. Note that from Eqs. (3) and (4), the energy change goes as the first power of the atomic-displacement parameter δ , whereas the elastic restoring forces go as δ^2 . This guarantees a finite macroscopic distortion below the magnetic-ordering temperature where the spins order collinearly. It also introduces a large crystalline anisotropy ($g_{\parallel} \neq g_{\perp}$) for the axis and magnitude of the atomic moments. A crystallographic distortion associated with an antiferromagnetic to paramagnetic transition may produce a first-order transition at T_N .

In Fe_{1-x}O and KFeF₃, there is a cubic to trigonal ($\alpha < 60^\circ$) transition with decreasing temperature at the Néel temperature T_N . However, whether the microscopic interstices are distorted to trigonal ($\alpha < 60^\circ$) or to tetragonal ($c/a > 1$) symmetry depends upon second-order considerations. Therefore, it is reasonable to assume that the cubic to tetragonal ($c/a > 1$) transition at T_N in RbFeF₃ is due to a Jahn-Teller stabilization in the presence of internal molecular fields. The only surprising feature is that the transition is second order and poorly defined.

Levinstein *et al.*⁸ have demonstrated that extensive twinning takes place in RbFeF₃ below T_N , the extent of the twinning increasing with the c/a ratio as T is decreased. This observation indicates that strong magnetoelastic coupling is present right through T_N , dynamically cooperative Jahn-Teller distortions occurring within regions of short-range magnetic order above T_N . Since adjacent regions of short-range order may have their spin axes aligned perpendicular, cooling through the Néel temperature introduces twin planes. Creation of these twin planes requires energy, so the temperature at which long-range magnetic order sets in depends upon the energy required to create twin planes for the relief of internal stresses created by the magnetoelastic coupling. This energy requirement varies from region to region within any real crystal, thereby leading to the spatial variation of T_N suggested by Wertzheim *et al.*¹

In oxides with the perovskite structure, distortions to orthorhombic symmetry are common.⁹ They represent a reduction in the anion coordination of the larger cation and can be correlated satisfactorily with the relative size and electronegativity of this cation. In the absence of a Jahn-Teller distortion, the general symmetry sequence with decreasing temperature in oxides is cubic → rhombohedral → orthorhombic. Although this sequence is not found in RbFeF₃, where a Jahn-Teller distortion is present, it is reasonable to assume that any orthorhombic symmetry has the $Pbnm$ space group of GdFeO₃.¹⁰ This symmetry permits the existence of a Dzialoshinskii vector \mathbf{D} parallel to the orthorhombic axis \mathbf{b}_0 , and hence a canting of the spins to produce weak ferromagnetism for certain combinations of magnetic order and spin direction. In particular, with type-G magnetic order, spins parallel to \mathbf{c}_0 may be

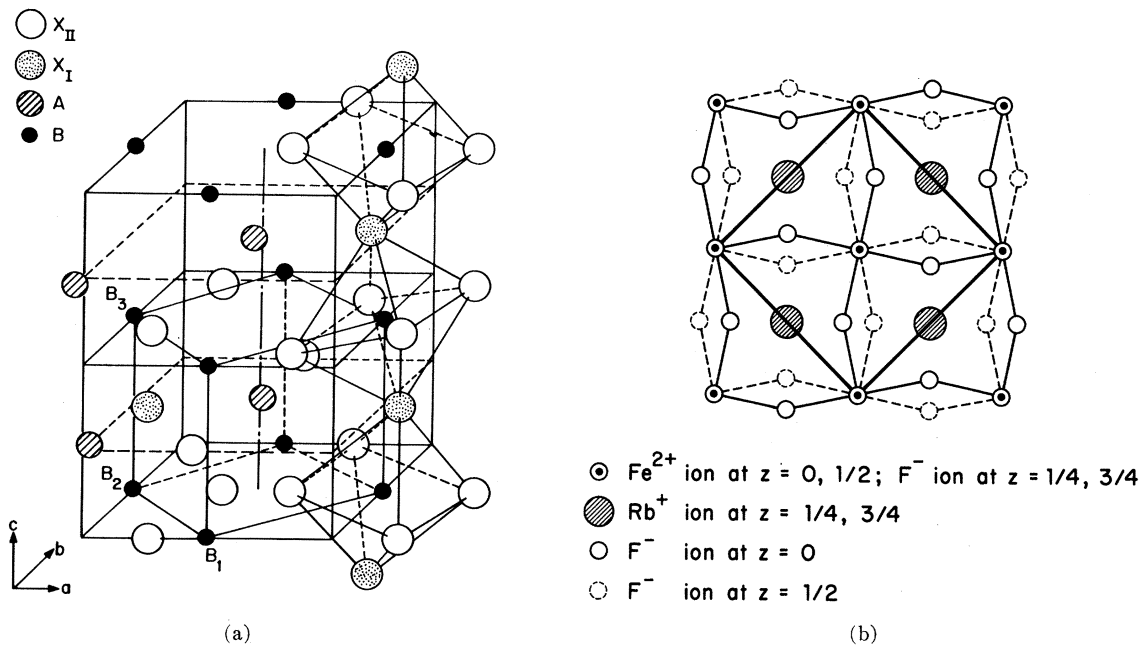


FIG. 2. Two Rb⁺-ion-induced distortions of the perovskite structure: (a) Orthorhombic *Pbnm*. (b) Tetragonal ($c_T = 2c_T$) projected on (001).

canted so as to give a net ferromagnetic moment parallel to \mathbf{a}_0 and spins parallel to $(\mathbf{a}_0 \pm \mathbf{b}_0)$ will cant in the \mathbf{a}_0 - \mathbf{c}_0 plane to give a net ferromagnetic moment parallel to \mathbf{c}_0 . This immediately provides a mechanism for the appearance of weak ferromagnetism below T_2 . Furthermore, Levinstein *et al.*⁸ have observed directly that at T_2 ferromagnetism is associated with the orthorhombic phase and that this ferromagnetic phase boundary moves across the twin planes of the tetragonal phase so as to include some regions having $\mathbf{c}_T \rightarrow \frac{1}{2}\mathbf{c}_0$ and others having $\mathbf{c}_T \rightarrow \frac{1}{2}(\mathbf{a}_0 + \mathbf{b}_0)$.

Since the RbFeF₃ crystals are heavily twinned below T_N , there are approximately equal volumes of material having \mathbf{c}_T directed along each of the three pseudocubic $\langle 100 \rangle$ axes. Although additional twinning may occur below T_2 , it was found that those twin planes associated with the orthorhombic distortion are mobile in applied magnetic fields.⁸ In fact, for $H_a > 0.5$ kOe, essentially all of these mobile twin planes are removed,⁴ so that the specimen appears macroscopically orthorhombic. Nevertheless, it still contains the twins due to the Jahn-Teller distortion. In those regions of the specimen where $\mathbf{c}_T \rightarrow \frac{1}{2}\mathbf{c}_0$, spin canting would give a spontaneous ferromagnetic moment σ_0^0 parallel to \mathbf{a}_0 , which is along a pseudocubic $\langle 110 \rangle$ axis. Where $\mathbf{c}_T \rightarrow \frac{1}{2}(\mathbf{a}_0 \pm \mathbf{b}_0)$, spin canting gives a spontaneous ferromagnetic moment $\sigma_0^0/\sqrt{2}$ parallel to \mathbf{c}_0 , which is along a pseudocubic $\langle 100 \rangle$ axis. This moment is reduced by $1/\sqrt{2}$ because only the component of the spin parallel to \mathbf{a}_0 contributes to the spin canting. Furthermore, it has been observed⁴ that

applied fields of 5 kOe are insufficient either to rotate the weak ferromagnetic moment more than about 2° from the easy axis of magnetization or to induce a spin flip, although they are sufficient to move twin planes associated with the orthorhombic phase. This model then suggests a net magnetization, after application of a field $H_a = 5$ kOe parallel to $[001]$,

$$\sigma^0 = \frac{1}{6}\sqrt{2} \{ (0, 0, 1) + (0, 0, 1) + (1, 1, 0) \} \sigma_0^0, \quad (6)$$

where the Miller indices refer to the pseudocubic unit cell, and the orthorhombic axes are

$$\mathbf{c}_0 \parallel (0, 0, 1), \mathbf{a}_0 \parallel \frac{1}{2}\sqrt{2}(1, 1, 0), \mathbf{b}_0 \parallel \frac{1}{2}\sqrt{2}(\bar{1}, 1, 0). \quad (7)$$

However, Gyorgy *et al.*⁴ have found that the torque curves for an "apparently single" crystal of RbFeF₃ give cubic symmetry with $\langle 100 \rangle$ easy axes and a $\cos\theta$ dependence. This observation is clearly incompatible with Eq. (6), which means that some modification of the model is required.

Modification of the model begins with the observation that the distortions to "orthorhombic" symmetry are much smaller than the Jahn-Teller distortion to tetragonal ($c/a > 1$) symmetry and that our assignment of the *Pbnm* space group was an assumption. In oxides, the orthorhombic symmetry *Pbnm* occurs where the larger cation is relatively small. It reduces the near-neighbor anion configuration about the larger cation from 12 to (5+2+5), as illustrated in Fig. 2(a). This

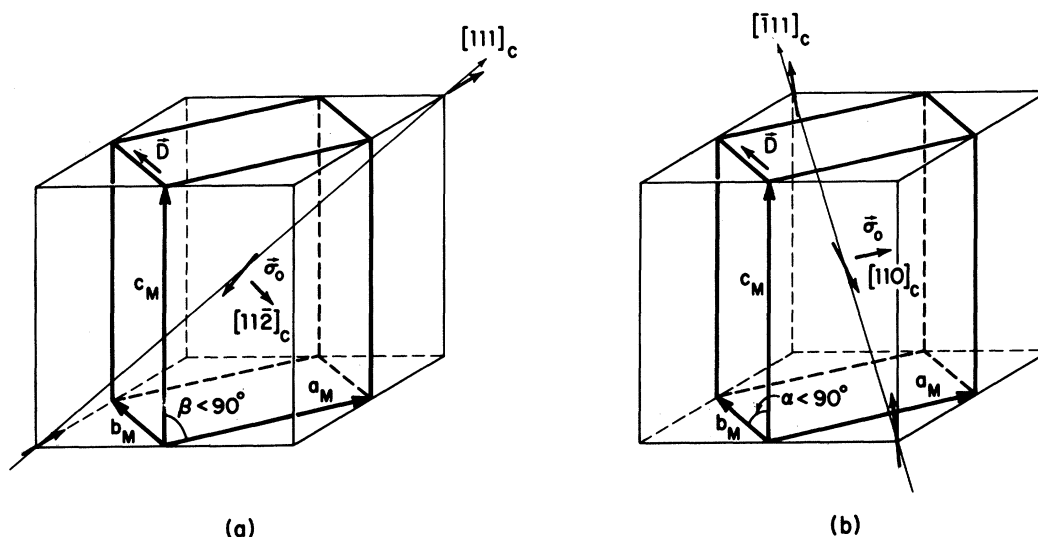


FIG. 3. Two rhombohedral Jahn-Teller distortions superposed on orthorhombic $Pbnm$ structure: (a) $\beta < 90^\circ$, (b) $\alpha < 90^\circ$.

permits the formation of shorter metal-anion bonds. In fluorides, on the other hand, the anion is much more ionic, and the anion configuration about the larger cation tends to be maximized, particularly in the case of a large cation like Rb^+ . These observations suggest that the distortions below T_2 are induced by the Jahn-Teller distortion below T_N , which reduces the anion configuration about a Rb^+ ion from 12 to $(4+8)$. A distortion that would increase this again to $(4+4+4)$, possibly approaching $(8+4)$, is shown in Fig. 2(b). Note that there is a doubling of each of the pseudocubic axes to form a new tetragonal unit cell having $\mathbf{c}_T' = 2\mathbf{c}_T$. This has a larger near-neighbor anion configuration about each Rb^+ ion than would the space group $Pbnm$ of Fig. 2(a). Therefore this would appear to be the more stable alternative. However, if the unique axis \mathbf{c}_T' crosses a twin plane, then it is perpendicular to \mathbf{c}_T in the twin. In this case the distortion of Fig. 2(b) would give a near-neighbor anion configuration about each Rb^+ ion that is reduced to $(2+2+8)$, which would not be competitive with the $Pbnm$ configuration of Fig. 2(a). Since the twin planes associated with the "orthorhombic" distortion below T_2 move across the twin planes due to the Jahn-Teller distortion, it seems more consistent to assume that where \mathbf{c}_T would transform to $\frac{1}{2}(\mathbf{a}_0 \pm \mathbf{b}_0)$, the symmetry is $Pbnm$ as illustrated in Fig. 2(a); that where \mathbf{c}_T would transform to $\frac{1}{2}\mathbf{c}_0$, it transforms instead to $\frac{1}{2}\mathbf{c}_T'$ to produce the symmetry of Fig. 2(b). The change of structure from that of Fig. 2(a) to that of Fig. 2(b) is sufficiently subtle that for small oxygen displacements the x-ray techniques that identify a specimen as macroscopically a "single crystal" below T_N would identify specimens subjected to external fields $H_a > 0.5$ kOe as "probably orthorhombic."

This model accounts nicely for four puzzling experimental findings. First, the Fe^{2+} ions in regions where $\mathbf{c}_T \rightarrow \frac{1}{2}\mathbf{c}_T'$ would experience internal fields different from those of Fe^{2+} ions in regions where $\mathbf{c}_T \rightarrow \frac{1}{2}(\mathbf{a}_0 \pm \mathbf{b}_0)$, thus giving rise to the two different Mössbauer spectra reported by Wertheim *et al.*¹ while permitting the weak ferromagnetism to be due to spin canting. Second, since there is no weak ferromagnetism associated with the symmetry of Fig. 2(b), the modified model changes Eq. (6) to

$$\sigma^{(0)} = \frac{1}{3}\sqrt{2}(0, 0, 1)\sigma_0^0, \quad (6')$$

which does agree with the experimental torque curves. Similarly, application of an $H_a > 0.5$ kOe parallel to $(0, 1, 0)$ or $(1, 0, 0)$ would create a $\sigma^{(0)} = (\frac{1}{3}\sqrt{2})\sigma_0^0$ parallel to these directions because of a switching of \mathbf{c}_0 from $(0, 0, 1)$ to $(0, 1, 0)$ or $(1, 0, 0)$. Thus the apparent cubic symmetry of a noncubic "crystal" is due to switching of a unique crystallographic axis in the applied field H_a . Such a switching is possible because the "orthorhombic" component of the distortion is induced by the large magnetostriction associated with the Jahn-Teller distortions, which do not switch. This does not contradict the finding⁴ from strain gauge measurements during switching, that the "c" axis does not follow σ , because only the small orthorhombic component of the distortion is involved. This component of the distortion has been observed directly by metallographic techniques to be switchable in fields $H_a > 0.5$ kOe.⁸ The "c" axis referred to above is essentially due to the Jahn-Teller component, which does not switch. Since the magnetic energy required to switch an "orthorhombic" \mathbf{c}_0 axis is only that needed to create and move a mobile twin plane, it may be 3 orders of

magnitude smaller than the latent heat at T_2 , as observed. Third, because switching is due to rotation of a unique crystallographic axis rather than to rotation of electron spins, the fact that the spins are rotated by less than 2.5° in an $H_a=16$ kOe can be reconciled with a torque curve that shows switching from a $[100]$ to an $[010]$ direction in the $H_a=5$ kOe.⁴ Fourth, because the "orthorhombic" distortion occurs to maximize the number of nearest neighbors at each Rb^+ ion, rather than to reduce the Rb-F bond length, a puckering that destroys the close-packed arrangement of RbF_3 layers expands the volume, which accords with our experimental results at T_2 .

Since the Jahn-Teller distortion may be to either tetragonal ($c/a > 1$) or rhombohedral ($\alpha < 60^\circ$) symmetry and since second-order terms in the energy stabilize the rhombohedral distortion in $\text{Fe}_{1-\beta}\text{O}$ and KFeF_3 , it is reasonable to anticipate a spin reorientation to the pseudocubic $\langle 111 \rangle$ axes at lowest temperatures. The small latent heat at T_1 is compatible with a simple spin-flop transition. Superposition of a rhombohedral Jahn-Teller distortion onto the orthorhombic crystal symmetry of Fig. 2(a) would indeed lower the symmetry to monoclinic (see Fig. 3), since the projection of the unique pseudocubic $\langle 111 \rangle$ axis onto the a_0 - b_0 plane would be parallel to either \mathbf{a}_0 or \mathbf{b}_0 . Thus $a_0, b_0, c_0 \rightarrow a_M, b_M, c_M$ and either $\alpha < 90^\circ$ or $\beta < 90^\circ$. Furthermore, the twin planes below T_2 would be both $\{110\}$, as in the interval $T_1 < T < T_N$, and $\{100\}$. Therefore below T_1 the original $\{110\}$ twin planes probably remain fixed, and an additional $\{100\}$ set may be added. Furthermore, note that there is no case where the unique axis due to the Jahn-Teller distortion coincides with an orthorhombic axis \mathbf{c}_0 , so that below T_1 the Rb^+ -ion-induced component of the distortion probably has orthorhombic symmetry $Pbnm$ with $\mathbf{D} \parallel \mathbf{b}_M$ over the entire volume of the crystal.

If the principal spin axis is parallel to the pseudocubic $[111]$ axis and the a_M, b_M, c_M axes correspond to pseudocubic $[110], [\bar{1}10], [001]$ axes, then a $\mathbf{D} \parallel \mathbf{b}_M$ produces a net ferromagnetic moment σ_0^M along the $[11\bar{2}]$ axis and $\beta < 90^\circ$, as illustrated in Fig. 3(a). On the other hand, if the spin axis is the $[\bar{1}11]$ axis as in Fig. 3(b), then the net moment is $\sigma_0^M/\sqrt{3}$ (since only the component parallel to \mathbf{c}_M is rotated by $\mathbf{D} \parallel \mathbf{b}_M$) along the $[110]$ axis and $\alpha < 90^\circ$. Again it is assumed that the applied field strengths are not strong enough to either

flip or rotate the principal spin axes, and the net magnetization, after application of an $H_a > 0.5$ kOe parallel to $[110]/\sqrt{2}$, becomes

$$\begin{aligned} \sigma^M &= (1/4\sqrt{6}) \\ &\times \{ (1, 1, \bar{2}) + (1, 1, 0) + (1, 1, 2) + (1, 1, 0) \} \sigma_0^M \\ &= (\sigma_0^M/\sqrt{3}) [(1, 1, 0)/\sqrt{2}]. \end{aligned} \quad (8)$$

Thus for an $H_a > 0.5$ kOe applied along any pseudocubic $\langle 110 \rangle$ axis, a $\sigma^M = \sigma_0^M/\sqrt{3}$ is created parallel to that $\langle 110 \rangle$ axis. Consequently in an $H_a = 5$ kOe, the monoclinic phase will appear cubic with the $\langle 110 \rangle$ axes as equivalent axes of easy magnetization, which is what has been found experimentally.⁴ Furthermore, those regions of the crystal having $\alpha < 90^\circ$ can in principle have a different internal field at the Fe^{2+} ions than those having $\beta < 90^\circ$, so that again two distinguishable Mössbauer spectra are possible, though the differences would be less pronounced than in the interval $T_1 < T < T_2$.

Finally, it is significant that

$$(\sigma_{110}^M/\sigma_{100}^O) = (\sqrt{\frac{3}{2}})(\sigma_0^M/\sigma_0^O) \approx \sqrt{\frac{3}{2}}, \quad (9)$$

which accounts nicely for the rise in the weak ferromagnetic moment on passing from the orthorhombic to the monoclinic phase. In fact the ratio $\sqrt{\frac{3}{2}}$ appears to be in reasonable quantitative agreement with the measurements of Testardi *et al.*² and with our observed ratio of 1.3.

In conclusion, the rather extraordinary properties of RbFeF_3 can be understood as an interesting interplay of three well-known phenomena: (i) a Jahn-Teller distortion below T_N that preserves the spin-orbit coupling, thus inducing a large magnetocrystalline coupling, (ii) an orthorhombic distortion due to ionic-size considerations that permits the existence of a Dzialoshinskii vector, and hence spin canting (except in those regions where \mathbf{c}_0 would be parallel to tetragonal \mathbf{c}_T axis due to a Jahn-Teller distortion), and (iii) a spin flop due to a change in the orientation of the Jahn-Teller distortion as a result of the temperature dependence of the elastic constants.

ACKNOWLEDGMENT

The RbFeF_3 crystal used in this study was kindly supplied to us by J. R. O'Connor.

† Work sponsored by the Department of the Air Force.

¹ G. K. Wertheim, H. J. Guggenheim, H. J. Williams, and D. N. E. Buchanan, *Phys. Rev.* **158**, 446 (1967).

² L. R. Testardi, H. J. Levinstein, and H. J. Guggenheim, *Phys. Rev. Letters* **19**, 503 (1967).

³ F. F. Y. Wang and M. Kestigian, *J. Appl. Phys.* **37**, 975 (1966).

⁴ E. M. Gyorgy, H. J. Levinstein, J. F. Dillon, Jr., and H. J. Guggenheim, *J. Appl. Phys.* **40**, 1599 (1969).

⁵ F. F. Y. Wang, D. E. Cox, and M. Kestigian, *Bull. Am. Phys. Soc.* **13**, 468 (1968).

⁶ N. Menyuk, J. A. Kafalas, K. Dwight, and J. B. Goodenough, *J. Appl. Phys.* **40**, 1324 (1969).

⁷ J. B. Goodenough, *Phys. Rev.* **171**, 466 (1968).

⁸ H. J. Levinstein, H. J. Guggenheim, and C. D. Capio, *Trans. AIME* **245**, 365 (1969).

⁹ J. B. Goodenough and J. M. Longo, *Landolt-Bornstein Tabellen, Neue Serie III/4a* (Springer-Verlag, Berlin, 1970), p. 126.

¹⁰ S. Geller, *J. Chem. Phys.* **24**, 1236 (1956).